ELSEVIER

Applied Ocean Research 27 (2005) 142–157

Applied Ocean Research

www.elsevier.com/locate/apor

Formation of walls of water in 'fully' nonlinear simulations

R.H. Gibbs [1], P.H. Taylor *

Department of Engineering Science, University of Oxford, Parks Road, Oxford OX1 3PG, UK

Received 19 May 2005; received in revised form 21 November 2005; accepted 24 November 2005
Available online 2 February 2006

Abstract

This paper analyses the spatial evolution of steep directionally spread transient wave groups on deep water and identifies key nonlinear dynamic processes in their formation. Sightings and field measurements of unexpectedly large 'freak' waves on the open ocean appear inconsistent with standard statistical distributions, but it has only recently become practical to study them via numerical experiments. The frequency focusing of many wave components, spread in both frequency and direction, provides a sufficient concentration of energy to trigger nonlinear effects. The evolution of these waves, based on a realistic model for the peak of an ocean spectrum, is computed by a 'fully' nonlinear pseudospectral scheme. The steepest wave groups form a prominent peak crest, which could be considered to be a 'wall of water'. The formation of this structure is controlled by the group properties of the wave field and results in rapid changes to the group shape relative to a linear solution. There is a dramatic contraction of the group along the mean wave direction, which appears to be balanced by a dramatic expansion of the group in the transverse direction. These processes appear to be consistent with third-order nonlinear wave–wave interactions.

Keywords: Directional spread; Focused wave groups; Freak waves; Near-resonant interactions; Nonlinear

1. Introduction

In recent years there has been increased interest in the possibility of unexpectedly large ocean waves, termed 'freak' or 'rogue' waves, inconsistent with standard statistical distributions. Seafarers have logged sightings of such waves for many years, and there are now field measurements to support their existence. On 1st January 1995, during a storm with significant wave height of 12 m, Statoil's 'Draupner' gas platform was struck by a wave of measured crest height 18.5 m, causing minor damage to equipment below the deck, [1]. Inspection of the time history of the surface elevation at the platform containing the large crest shows that the depth of the preceding trough was only 7.5 m: there was no obvious indication of the extreme wave about to strike. The Schiehallion FPSO, a BP Amoco vessel moored in the North Atlantic, was hit by a large wave on 9th November 1998. The impact pushed in bow plating at 20 m above the mean water level, during a sea state with an estimated significant wave height of 14 m. In the autumn of 1995, the ship's master of the Queen Elizabeth 2 recalls seeing 'a wall of water for a couple of minutes' during a severe storm off Newfoundland. These examples highlight some characteristics commonly used to describe 'freak' waves.

Recent field measurements show that ocean wave spectra are broadbanded and highly directional, and so large ocean waves may be expected to be strongly dispersive. An analysis of field data by Jonathan et al. [2], measured at the Tern platform in the northern North Sea, suggests that even the largest wave events are well modelled by a second-order solution applied to the underlying frequency spectrum. These findings imply that 'freak' waves are likely to be rare, and that strong nonlinear effects are needed to trigger their formation. Whether the existence of 'freak' waves requires modifications to standard offshore design methods remains to be seen. Although there is no widely accepted model for the formation of 'freak' waves, a recent review of possible physical mechanisms leading to 'rogue' waves has been presented by Kharif and Pelinovsky [3]; this review concentrates on model evolution equations. In contrast, our paper gives numerical simulations of the full water wave equations.

There has been considerable study of the nonlinear dynamics of gravity waves on deep water in the last forty years. The lowest order nonlinear mechanisms that can alter the dynamics of a group of waves are the third-order resonant interactions of Phillips [4], which permit certain combinations

* Corresponding author. Tel.: +44 1865 273198; fax: +44 1865 273010.
E-mail address: paul.taylor@eng.ox.ac.uk (P.H. Taylor).
[1] Present address: Division of Civil Engineering, University of Dundee, Dundee DD1 4HN, UK.

0141-1187/$ - see front matter © 2005 Elsevier Ltd. All rights reserved.
doi:10.1016/j.apor.2005.11.009

of three wave components to transfer energy to a fourth component. However, Lighthill [5] was the first to show, by Whitham's averaged Lagrangian technique, how nonlinear dynamic effects could increase the peak amplitude and distort the shape of a slowly varying wavetrain of finite amplitude. He was also the first to note that, for a wave group with shorter waves ahead of a central peak in amplitude and longer waves behind (the frequency focusing of a wave group), linear frequency dispersion and nonlinear amplitude dispersion can combine to cause a local enhancement of the peak amplitude. This third-order effect was shown by Benjamin and Feir [6] to give rise to the instability of a regular wavetrain to long wave modulations. This is a narrowbanded process and is likely to be important in the formation of large waves as much of the energy in ocean wave spectra is concentrated close to a peak. The simplest mathematical model, relevant to modelling a spectral peak, that includes these effects is the nonlinear Schrödinger equation (NLS), which describes the envelope modulations of weakly nonlinear surface gravity waves on deep water (reviews of known solutions are given by Peregrine [7], and Dysthe and Trulsen [8]). An extensive review of the properties of the NLS and instabilities that give rise to energy transfer in ocean spectra is given by Yuen and Lake [9]. Several extensions have been made to the NLS model [10–12] with regard to the problems of energy leakage and bandwidth constraints, which have made it more suited to modelling on spread seas. Dysthe et al. [13] have subsequently used these models to study random wave spectra, as mentioned in Section 4. However, only a few investigators have used such models to consider the shape taken by isolated extreme spread sea waves. Lo and Mei [14] showed that an initial wave group elongated along the mean wave direction spreads in the transverse direction to form a ridge, whereas the behaviour of an initial group elongated in the transverse direction is dominated by group splitting. More recently, Osborne, Onorato and Serio [15] demonstrated that unstable modes in two horizontal dimensions can cause waves much larger than the background.

The largest ocean waves are probably highly transient, arising from a random background where both the wave nonlinearity and directionality significantly affect the local properties of the extreme event [16]. The frequency focusing of a wave group, whereby many wave components have maxima that coincide at a particular point in space and time, provides a model that is consistent with the description of a transient event and produces a sufficient concentration of energy to trigger nonlinear dynamic effects. The unidirectional, 'fully' nonlinear numerical simulations of Taylor and Haagsma [17] showed that as a group focuses it becomes narrower and much higher than linear theory would predict. This extra elevation was found to be up to 30% greater than the corresponding linear solution for narrowbanded groups in the wave flume experiments of Baldock et al. [18]. In both the experimental and modelling work the extra elevation increases with the input amplitude of the group, but decreases with its bandwidth. Such behaviour shares features in common with the algebraic breather solutions to the NLS equation [7,8]. Detailed comparisons of 'fully' nonlinear simulations for both unidirectional and spread sea groups with the results from the NLS equation will be given in a future paper.

The wave basin experiments of Johannessen and Swan [16] showed that, for fixed initial input amplitudes, even a small amount of directional spreading leads to a significant reduction in the extra elevation of a focused wave group, which is now almost completely captured by a second-order model. They also found local directionality changes requiring a greater initial input amplitude to initiate wave breaking at the nonlinear focus as compared to unidirectional groups. These results were confirmed by the numerical simulations of Bateman [19] and Johannessen and Swan [20]. Although there seems to be nothing extraordinary about the maximum surface elevation attained in these experiments, the authors did show that significant energy is still transferred to high wavenumber components well beyond the linear spectral range. This wave energy was shown to be freely propagating by the 'fully' nonlinear numerical replication of these experiments by Johannessen and Swan [20]. Large energy transfers to high wavenumbers have also been observed in unidirectional extreme waves [18], where they are consistent with a contraction of the group, but their effect on the shape of a spread sea group is unclear. As descriptions of 'freak' waves refer to spatial characteristics, a detailed analysis of the spatial evolution of focused wave groups on a spread sea is required in order to investigate the consequences of these large energy transfers.

Our aim is to present some numerical simulations of steep focused wave groups on deep water and show how the shape of these waves alters due to nonlinear dynamics. The most nonlinear wave groups form a prominent steep peak crest with a near constant elevation more than one wavelength wide (200 m in our simulation) in the transverse direction (crestline). This wall-like shape is shown in Fig. 1 for an input wave steepness (Ak_p) of 0.3. Note that we refer to wave groups by their input steepness, Ak_p—where A is the linear focused amplitude and k_p is the wavenumber of the peak of the initial unidirectional spectrum, which is the steepness of the focused wave group that would form under linear dynamics. The analysis of the formation and subsequent evolution of this extreme wave event is the main concern of this paper.

2. Numerical method

2.1. Numerical scheme

The formation of extreme deep water waves is studied by the frequency and directional focusing of many wave components. It is assumed that such events may be modelled on an incompressible inviscid irrotational fluid so that the motion is governed by Laplace's equation for the velocity potential. In addition there are no underlying currents and the effects of surface tension and the interaction of the air with the water surface are neglected. This allows the specification of two free surface boundary conditions, which lead to the explicit expressions for the time derivatives of the surface elevation, $\eta(x,y,t)$, and the velocity potential, $\phi(x,y,z,t)$,

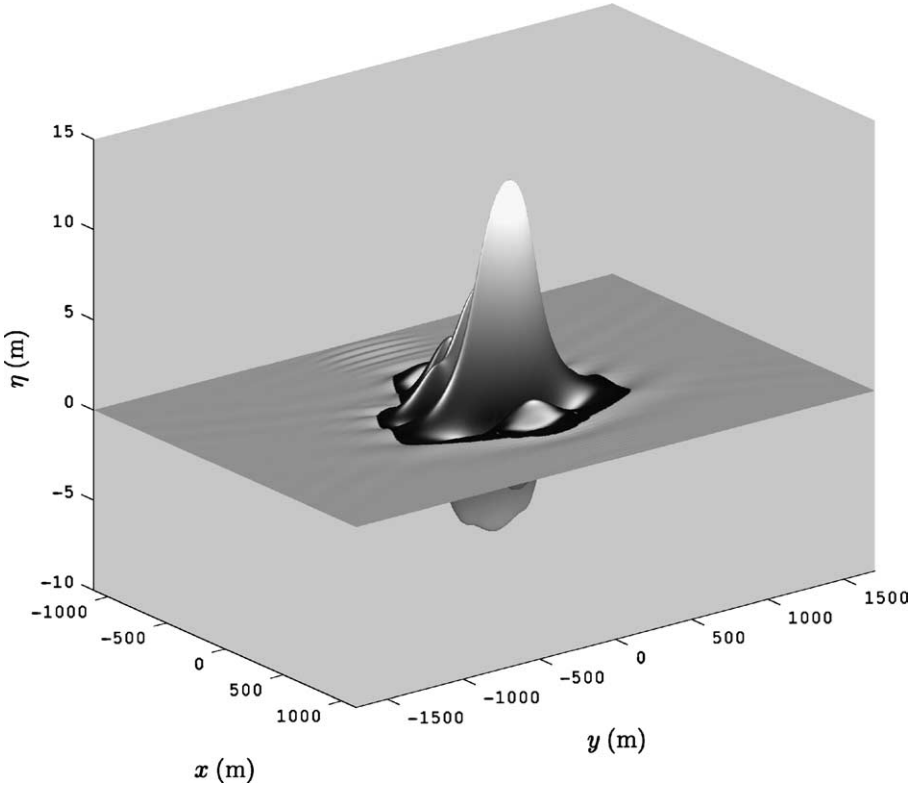

Fig. 1. Frontal view of surface elevation at point of nonlinear focus ($t=1.3T_p$), $Ak_p=0.3$. The frame of reference is moving at the linear group velocity. The surface has been shaded above a threshold of 0.15 m and the vertical scale enhanced by a factor of 100 with respect to the horizontal scales.

$$\eta_t = \phi_z - \phi_x\eta_x - \phi_y\eta_y \tag{1}$$

$$\phi_t = -\frac{1}{2}(\phi_x^2 + \phi_y^2 + \phi_z^2) - g\eta. \tag{2}$$

Given a suitable initial condition, the equations above may be time-stepped to give the evolution of the water surface. However, their evaluation requires computation of the tangential and normal derivatives of ϕ on the surface. For calculation of the normal derivative, knowledge of ϕ in the fluid interior is necessary and becomes the crucial step in any accurate and efficient time evolution scheme. Craig and Sulem [21] showed that a Dirichlet–Neumann operator (G-operator) could be used for the accurate conversion of the velocity potential on the surface, ϕ^s, into its normal derivative on the surface. This approach was extended to the simulation of directional seas by Bateman et al. [22]. They defined the G-operator as

$$G(\eta)\phi^s = \phi_z. \tag{3}$$

The surface elevation and velocity potential are represented by Fourier series and the wave motion is restricted to a domain that is periodic in both horizontal dimensions, x and y. The surface velocity potential and its vertical derivative are expanded as Taylor series about the mean sea level and, with a Taylor series expansion of the G-operator, are substituted into Eq. (3). By comparing terms of the same degree of homogeneity, a recursive formula for the G-operator is obtained, which has its first three terms given by

$$G_0 = D\tanh(Dh) \tag{4a}$$

$$G_1 = \eta D^2 - D\tanh(Dh)\eta D\tanh(Dh) \tag{4b}$$

$$\begin{aligned} G_2 = {} & \frac{1}{2}\eta^2 D^2 D\tanh(Dh) - \eta D^2\eta D\tanh(Dh) \\ & -\frac{1}{2}D\tanh(Dh)\eta^2 D^2 \\ & + D\tanh(Dh)\eta D\tanh(Dh)\eta D\tanh(Dh), \end{aligned} \tag{4c}$$

where h is the uniform depth, $D=-i\partial/\partial\sqrt{x^2+y^2}$ is a complex radial derivative operator and $\tanh(Dh)\to\mathrm{sgn}(D)$ in the limit of infinite depth. The G-operator contains both spatial and spectral information and so is evaluated by performing multiplications in physical space and differentiations in wavenumber space. The FFT may be used for the frequent switching between physical and spectral space, which gives a method that is $O(n\log n)$. As this is a pseudospectral method, the surface elevation must be a single valued function of the horizontal coordinates and so simulations are restricted to the early stages of wave breaking before the surface becomes vertical. Bateman et al. [22] validated the scheme against the high quality wave basin data of Johannessen and Swan [16] for groups with a range of bandwidths, directional spreading, and steepness up to the physical breaking limit. The scheme was shown to be efficient, robust and suitable, even on a PC, for modelling broadbanded, highly nonlinear directional sea states.

2.2. Initial spectral model

An initial condition is now required that will evolve over a given time to form an extreme wave. The average shape of an extreme in a random sea is a useful concept and Lindgren [23] showed that, in a linear random Gaussian signal, the average shape of a large positive or negative peak tends to the scaled autocorrelation function of the signal. In a series of papers from 1981 onwards (see for example [24–26]) Boccotti developed similar ideas in the context of wind waves, showing that the autocorrelation function matches the average shape of a large crest in both time and space. This idea was transferred into offshore engineering practice by Tromans et al. [27], where it is now known as NewWave. An important feature of Lindgren and Boccotti's model is the link between an averaged local extreme event and the global properties of the sea state, since the autocorrelation function is the Fourier transform of the underlying power spectrum. Both temporal and spatial aspects of the model have been validated against field data for waves in the Straits of Messina [25] and for large deep water waves in severe winter storms in the northern North Sea [28]. In the context of this paper we assume that the early stages of the formation of an extreme event are dominated by linear dispersion. Thus, the shape of our initial condition matches that of a scaled autocorrelation function in space at twenty wave periods before focus. Thereafter, as the wave group approaches focus, nonlinear effects are likely to become important if the group is sufficiently steep. Hence, we use the 'fully' nonlinear numerical scheme to follow the subsequent evolution of the wave group.

A common method in offshore engineering of modelling a directional frequency spectrum, $F(\omega,\theta)$, is as the simple product of a unidirectional spectrum, $S(\omega)$, and a spreading function, $D(\theta)$, where ω is the radian frequency and θ the direction of wave propagation,

$$F(\omega,\theta) = S(\omega)D(\theta). \tag{5}$$

The JONSWAP spectrum, derived from field measurements [29], is considered to be a suitable description of a broadbanded ocean spectrum in a fetch-limited sea. However, much of the energy of this spectrum is concentrated in a narrow range of frequencies around its peak and so we consider the modelling of components close to the peak of the spectrum only as an important first step in understanding the behaviour of directional broadbanded events. We use a Gaussian function for such a model

$$S(k) = \exp\left(\frac{-(k-k_\mathrm{p})^2}{2k_\mathrm{w}^2}\right), \tag{6}$$

where k is the wavenumber, k_p is the wavenumber corresponding to the position of the peak of the initial linear spectrum and k_w is the spectral width. We set $k_\mathrm{w}=0.004606\ \mathrm{m}^{-1}$, so that $S(k)$ given in Eq. (6) (when considered in terms of ω) fits the shape of the JONSWAP peak with a peak enhancement factor of $\gamma=3.3$ and defines $S(\omega)$ required by Eq. (5).

Donelan et al. [30] investigated the amount of spreading in high quality wind generated wave data recorded on Lake Ontario and found a low degree of spreading at the spectral peak, which increased with frequency. A comparison of their proposed spreading distribution with a wrapped normal Gaussian distribution suggests an rms spreading parameter of 20° at the frequency of the spectral peak, increasing to 30° at 1.4 times the frequency of the spectral peak. An analysis of directional ocean wave spectra by Ewans [31], measured off the west coast of New Zealand for a large range of wind and wave conditions, showed that for frequency components below twice the frequency of the spectral peak the spreading is less than 20°, whereas the higher frequencies are considerably more spread. These two studies suggest that the use of a wrapped normal Gaussian distribution with a constant rms spreading parameter, σ, of 15° will give realistic spreading for our spectral peak model, $D(\theta)$. We note that $F(\omega,\theta)$ for our spectral peak model is the product of two Gaussian functions, so the surface elevation of the focused linear event can be approximated as

$$\eta(x,y) = A\mathrm{e}^{-(1/2)S_x^2x^2}\mathrm{e}^{-(1/2)S_y^2y^2}\cos(k_\mathrm{p}x). \tag{7}$$

Thus, for narrow bandwidths the spatial bandwidth, S_x, is equivalent to the spectral width of the underlying unidirectional spectrum and the spatial bandwidth, S_y, is related to the rms spreading angle in radians, σ_rms, by $S_y=\sigma_\mathrm{rms}k_\mathrm{p}$. These relationships are valid for the wave groups considered in this paper, as the specified initial conditions are sufficiently narrow banded for Eq. (7) to be an excellent approximation to the shape of the linear focused NewWave groups.

The NewWave model with a wave power spectrum given by Eqs. (5) and (6) defines the initial amplitudes of the individual wave components in our simulations. We use the linear dispersion relationship ($\omega^2=|k|g$) to specify the phases of the individual wave components at twenty time periods before the linear focus, such that under linear dynamics all the wave components would have maxima coinciding at the spatial point $x=y=0$ at the time $t=0$. Thus, our initial condition leads to an event that is both direction and frequency focused.

2.3. Validation of the results

The area of ocean in the assumed periodic computational domain is 3.6 km in the mean wave direction by 5.8 km in the transverse direction, with 256 spatial points in each direction. For adequate resolution of the initial wave spectrum the spectral peak is placed at a wavenumber $k_\mathrm{p}=16k_0=0.02796\ \mathrm{m}^{-1}$ (corresponding to a wavelength of 225 m and a time period of $T_\mathrm{p}=12$ s), where k_0 is the wavenumber corresponding to the longest wavelength modelled in the x-direction. Therefore the highest wavenumber included in the simulation is at eight times the wavenumber of the spectral peak. The simulations are performed with a fifth-order expansion of the G-operator, although the results have also been checked with a seventh-order expansion, this allows accurate resolution of all fifth-order nonlinear interactions. The simulation is started 20 time periods (240 s) before the linear focus so that a linear model, corrected

for the second-order bound wave terms of Longuet-Higgins [32] provides a sufficiently accurate description of the surface at a time when the long-term effects of resonant interactions are assumed negligible. At this early time the dispersed group possesses only small bound wave corrections so omission of the third and higher order terms in the definition of the initial condition is acceptable. The subsequent evolution is of course 'fully' nonlinear. Several checks have been made to establish the integrity of the results. As there is no energy input or dissipation in the scheme the conservation of the total energy in the domain is monitored and results are presented only for cases with a non-physical variation in the total energy of less than 0.5%. The reversibility of the simulations is verified by using the values of the surface elevation and surface velocity potential at the end of one run as the initial conditions of a second run, which is stepped backwards in time to the original initial condition. In none of the simulations reported in this paper was there any wave breaking (which breaks the scheme). Previous simulations by Bateman [19] have shown that simulations are accurate up to the onset of breaking. Indeed Bateman's comparison with the experiments of Johannessen and Swan [16] suggest that the scheme can be used to predict the onset of breaking based on the vertical acceleration of the fluid particles.

3. Spatial evolution of spectral peak

3.1. Shape of sea surface

There are striking differences between the shape of the linear and nonlinear focused events. We define the focused event as the point in time when the peak surface elevation is a maximum with respect to the entire simulation. Under linear evolution the initially well dispersed wave group (Fig. 2(a)) forms a focused event, at $t=0$, that has a line of symmetry along a transverse direction and has its peak crest at the centre of the group (Fig. 2(b)). This crest is 10.7 m high and is preceded by a deep trough and a fairly high crest. In contrast, under nonlinear evolution the wave group forms an event, at $t=1.3T_p$, that is highly asymmetrical about a transverse direction with the peak crest moved to the front of the group (Fig. 1). This crest is 12.8 m high, but is preceded by a relatively shallow trough, which is only just visible in Fig. 1, and a low crest. The deep trough seen in Fig. 1 is directly behind the peak crest. The prominence of this peak crest shares features with the shapes of the modulational instabilities of the two-dimensional NLS equation reported by Osborne et al. [15] and Kharif and Pelinovsky [3]. Although the peak crest of the nonlinear event is only slightly higher than the linear one, its length in the transverse direction is much greater and it has a locally more planar front than the linear event. The subsequent evolution of the spatial structure of the wave group is shown in Fig. 3. The height and transverse width of the peak crest of the nonlinear event, with minimal preceding wave structure, are highly suggestive of a 'wall of water'.

These features of the peak crest persist for several time periods beyond the nonlinear focus, long after it might be expected that linear dispersion would cause the group to fall apart. This is seen in Fig. 3(d), (h) and (l) at two, four and six time periods after the nonlinear focus respectively, when the peak crest within the group attains values of 12.6, 12.0 and 11.2 m respectively (the peak crest coincides with the maximum of the wave group envelope at these times). We note that the linear focused amplitude is 10.7 m, a value exceeded by the peak crest that forms six time periods after the nonlinear focus. Indeed over the entire evolution the linear focused crest is exceeded in our 'fully' nonlinear simulation for more than 10 wave periods. Ahead of the peak crest the wave structure, which was of a low level at the focus time, almost disappears. The peak crest continues to widen in the transverse direction, as the group evolves from the focus point, and yet still has a locally fairly planar front.

The persistence of the focused wave group can perhaps be related to the observation of the ship's master of the Queen Elizabeth 2. Assuming the focused group could form in a random sea, elongated extreme crests might be visible for perhaps 8 wave periods from the ship's bridge. With a wave period of ∼15 s this corresponds to 2 min — compatible with the observation. It should be noted though that in this time four crests would pass through the extreme wave group leading to the 'beating' seen in Fig. 3.

Dramatic changes also take place behind the peak crest with evidence of two nonlinear processes: group splitting along the

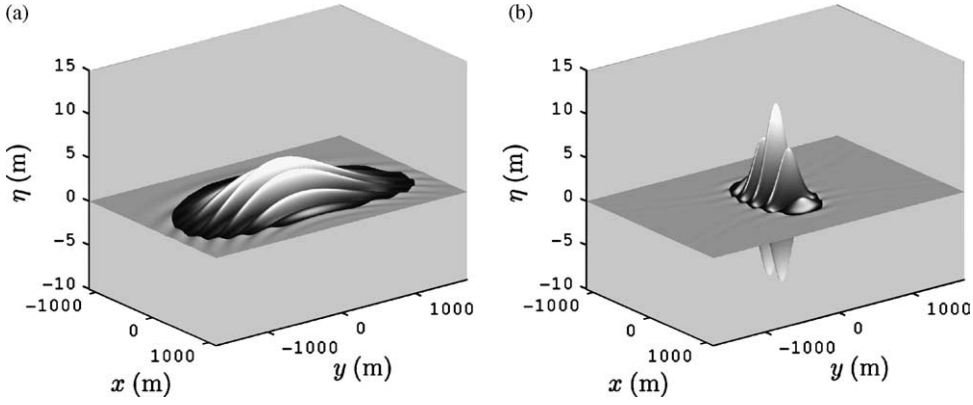

Fig. 2. Linear surface elevation, $Ak_p=0.3$: (a) $t=-20T_p$; (b) $t=0$ (linear focus). The frame of reference is moving at the linear group velocity. The surface has been shaded above a threshold of 0.15 m and the vertical scale enhanced by a factor of 100 with respect to the horizontal scales.

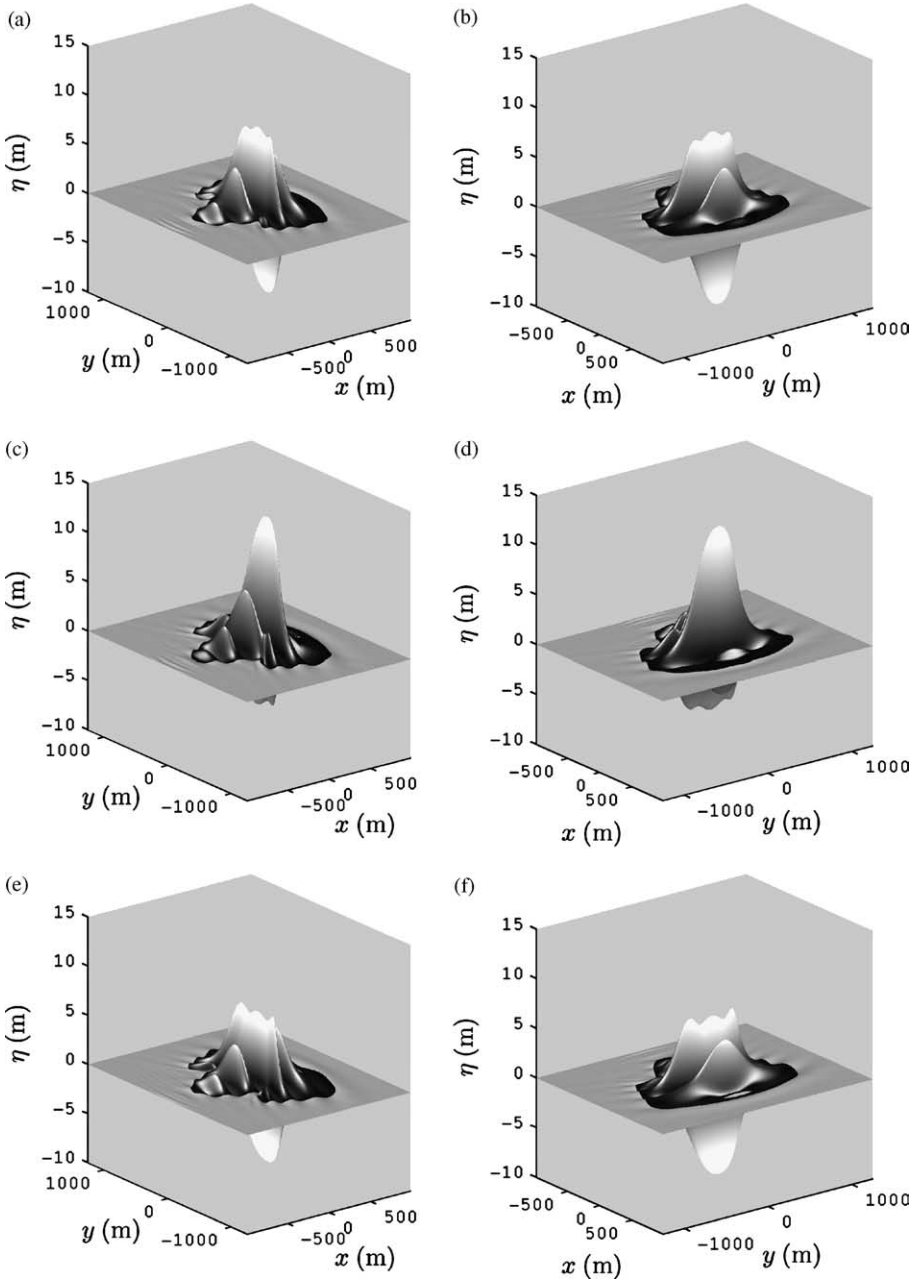

Fig. 3. Nonlinear surface elevation, $Ak_p=0.3$: (a), (b) $t=2.3T_p$; (c), (d) $t=3.2T_p$; (e), (f) $t=4.2T_p$; (g), (h) $t=5.2T_p$; (i), (j) $t=6.1T_p$; (k), (l) $t=7.1T_p$. The left hand column gives the rear view and the right hand column gives the frontal view of the group. The frame of reference is moving at the linear group velocity. The surface has been shaded above a threshold of 0.15 m and the vertical scale enhanced by a factor of 100 with respect to the horizontal scales.

mean wave direction and new wave structure travelling at an angle to the mean wave direction. These processes may be identified by tracing how the crest directly behind the peak crest of the nonlinear focus event (Fig. 4) evolves with time (Fig. 3). In Fig. 4 this crest is actually formed from three partially overlapping waves, which give the appearance of a central crest with two shoulders. At one time period after focus the central crest is slightly in front and higher than the two outer crests (seen from the three local maxima on the highest wave in Fig. 3(a)). Two time periods later the two outer crests are slightly in front of the central crest, which is now lower than these two crests (Fig. 3(e)). The two outer crests move further ahead of the central crest after another two time periods and there is clear definition between the three distinct waves (Fig. 3(i)). The height of this central crest is seen to decrease with time relative to the crest directly in front of it on the centre line of the group (Fig. 3(b), (f) and (j)). However, for a single group of waves all the crests behind the peak crest are rising and all the crests in front of the peak crest are falling, therefore Fig. 3 shows the splitting of the group along the mean wave direction. New wave structure develops from the nonlinear focus event, which is seen by tracing the evolution of the shoulders on the crest directly behind the peak crest (Fig. 4) in Fig. 3(c), (g) and (k). At the nonlinear focus the shoulders are level with the central crest directly behind the peak crest, but are at an

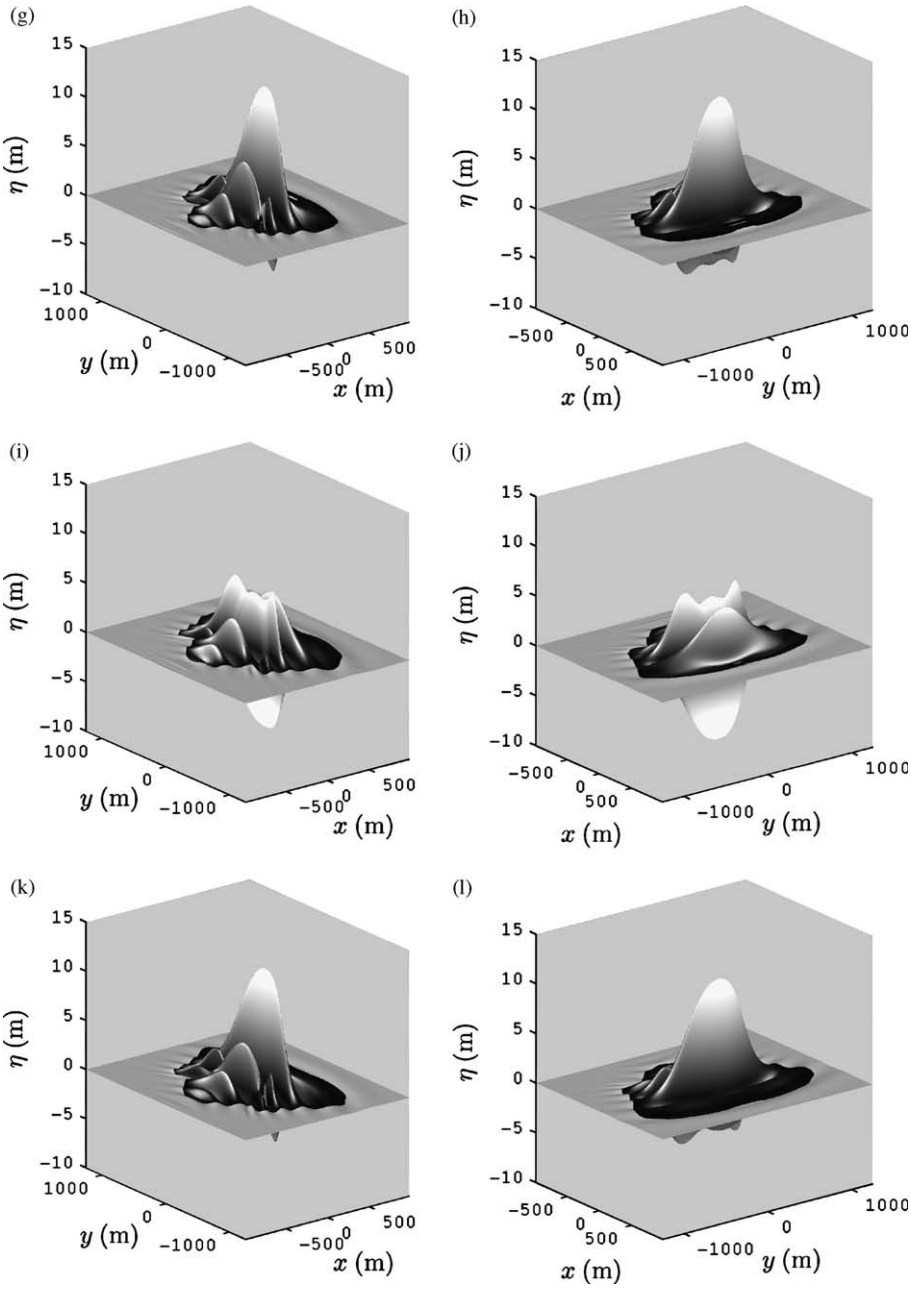

Fig. 3 (*continued*)

angle to the mean wave direction. The two outer crests forming these shoulders gradually separate from and overtake the central crest. In Fig. 3(g) and (k) these two outer crests have following crests, which are about to pass through the next crest on the centre line of the group. This new structure on the outer edge of the group is interleaved with the crests travelling in the mean wave direction and it is this structure which rises up from the sides to form the new peak crest at the front of the main group. Contour plots of the nonlinear surface elevation at three times after focus (Fig. 5) show that the new wave structure is travelling at about 30° to the mean wave direction and has shorter wavelength than the waves travelling along the centre line. This suggests that this wave structure is associated with energy transferred to wavenumbers higher than the spectral peak.

3.2. Visualizing changes to group shape

As the nonlinear event forms there is a dramatic contraction of the group, local to the peak crest. This is seen in Fig. 6 by considering vertical cross-sections through the wave group along the mean wave direction. The wave group exhibits essentially linear behaviour during the first 10 time periods of the nonlinear evolution. Rapid changes take place to the group in the following 10 time periods, up to the focus point, leading to strong differences between the nonlinear focused event (Fig. 6(a)) and the symmetric linear focused event. The nonlinear evolution results in a prominent peak crest close to the front of the wave group. This crest is considerably steeper and is much narrower than the peak crest in the linear focused

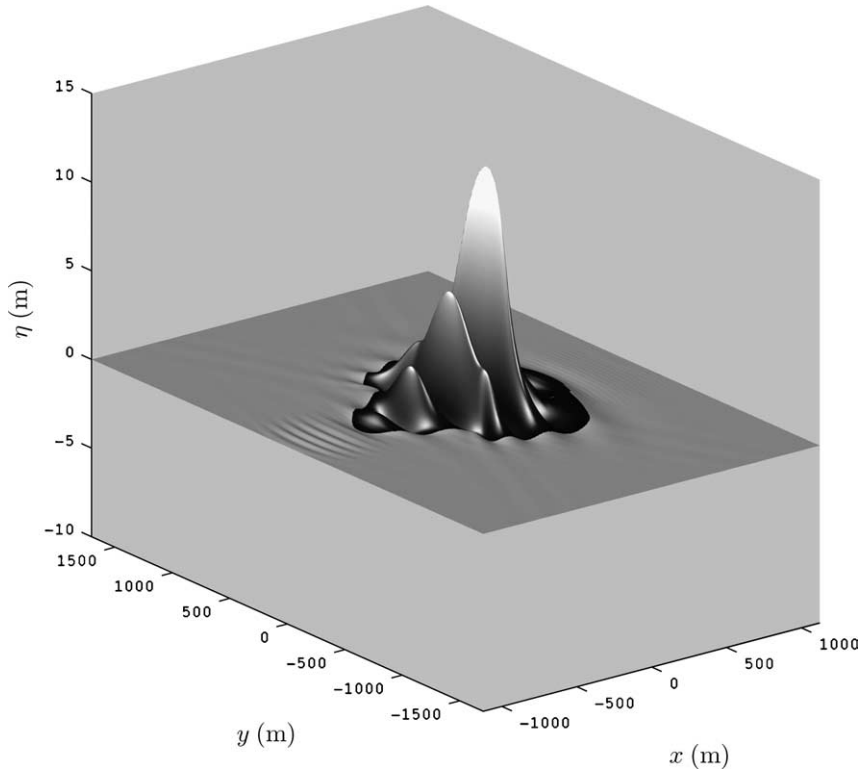

Fig. 4. Rear view of surface elevation at point of nonlinear focus, $Ak_p=0.3$. The frame of reference is moving at the linear group velocity. The surface has been shaded above a threshold of 0.15 m and the vertical scale enhanced by a factor of 100 with respect to the horizontal scales.

wave group. A measure of this local contraction in the mean wave direction may be given by the distance between the zero crossing points either side of the peak crest, which for the linear peak crest is 113.0 m and for the nonlinear peak crest is only 84.4 m. This contraction of 25% could be merely due to the presence of bound wave structure, which makes crests taller and spikier, and troughs less deep and more rounded. However, a signal constructed by the differencing of the crest-focused and trough-focused signals (Eq. (10)) gives 95.1 m for the same measure and so this contraction is not a second order effect. There are also strong differences in the wave structure ahead of the peak crest, which for the nonlinear event gives little warning of the following peak crest. The trough ahead of the nonlinear peak crest is only 4.0 m deep and the crest in front of this trough a mere 1.1 m high (Fig. 6(a)). The highly asymmetrical shape of the nonlinear focused wave group suggests that not all of the wave components are in phase. Although a relatively narrow band of wave components has been specified for the initial condition, it is clear that a more select collection of wave components actually take part in the processes that form the extreme event. The evolution after the nonlinear focused event is also striking, since many of the features in Fig. 6(a) persist 10

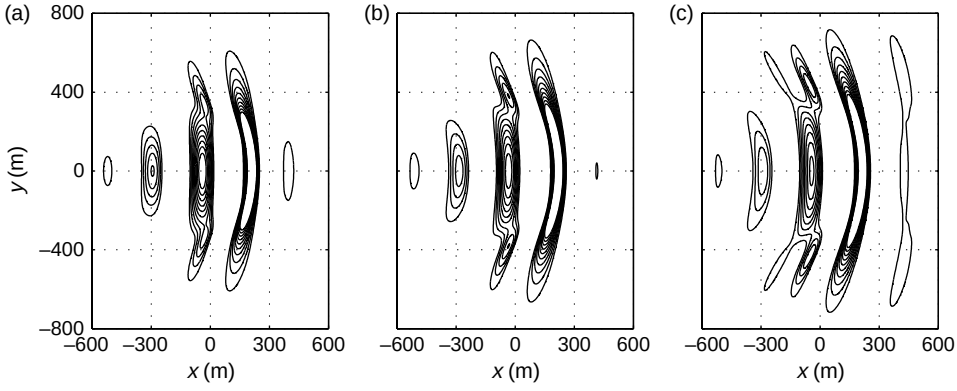

Fig. 5. Amplitude contours of the nonlinear surface elevation, $Ak_p=0.3$: (a) $t=3.2T_p$; (b) $t=5.2T_p$; (c) $t=7.1T_p$. The contours are given in 0.5 m intervals above mean sea level starting at $\eta=0.5$ m. The frame of reference is moving at the linear group velocity.

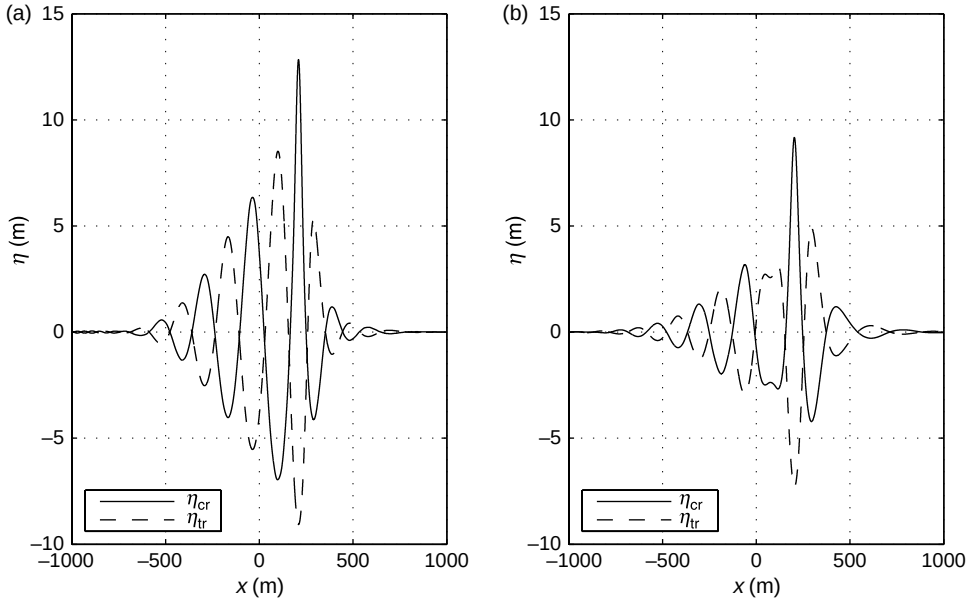

Fig. 6. Cross-section through the nonlinear wave group showing the surface elevation along the mean wave direction for the crest-focused event, η_{cr}, and the trough-focused event, η_{tr}, $Ak_p=0.3$: (a) $t=1.3T_p$; (b) $t=10.9T_p$. The frame of reference is moving at the linear group velocity.

time periods later in Fig. 6(b) at a time when linear dispersion might be expected to dominate the behaviour of the group. The peak crest is still rather steep, tall (50% higher than a linear prediction) and the heights of its preceding waves are almost unchanged compared to the nonlinear focused event.

The profile of the isolated crest in Fig. 6(b) is similar to that arising from modulational instability of a Stokes wave simulated by Dyachenko and Zakharov [33]. Their simulation is unidirectional and their initial condition is very narrow-banded. Thus, the dynamics of their waves are dominated by nonlinearity acting along a line. In contrast, the formation of our extreme event is at least initially dominated by linear dispersion, both in frequency and direction. However, it is interesting that, at least locally, comparable extreme wave events occur from very different initial conditions.

There is also clear evidence, seen from the double-peaked trough in the centre of Fig. 6(b), of the group beginning to split into two along the mean wave direction, as the waves that did not participate in the focused event are left behind the peak crest. Similar behaviour has been observed by Lo and Mei [14] in their numerical simulations of the two-dimensional NLS equation. The details of this splitting are presumably very sensitive to the details of the initial condition—unlike the formation of the main wave group, extended along the crests and contracted along the direction of wave propagation.

The simulation of the formation of a focused event with a deep trough at the centre of the group is useful in understanding the processes involved in the formation of a tall crest. A focused trough event, η_{tr}, is initiated by a linear input that is π radians out of phase, i.e. inverted, compared to that required to form a focused crest, η_{cr}. A remarkable feature of the nonlinear evolution in forming an extreme trough is that its global behaviour is effectively identical to that for the formation of an extreme crest, even for steep events close to breaking. The troughs in the trough-focused simulation are aligned, in space and time, with the crests of the crest-focused simulation and vice versa (Fig. 6(a) and (b)) throughout the simulation. This feature of crest-focused and trough-focused evolution has been seen in the wave basin experiments of Johannessen and Swan [16] and in the numerical spread sea simulations of Bateman [19]. For wave groups that evolve linearly this behaviour is obvious, but it is an important feature of nonlinear evolution given the different local shapes of the two extreme events. Therefore the formation of an extreme event is dependent on the group properties of the wave field, such as amplitude and shape, and not the absolute phasing of the waves within the group. A general fourth-order Stokes-like perturbation expansion for a crest-focused wave group, where all the amplitude components, a, are positive and assumed to be slowly varying with time and the interaction coefficients are given by c_{ij}, c_{ijk}, etc., would be of the form

$$\eta_{cr} = \sum_i a_i + \sum_{i,j} c_{ij}a_i a_j + \sum_{i,j,k} c_{ijk}a_i a_j a_k + \sum_{i,j,k,l} c_{ijkl}a_i a_j a_k a_l. \quad (8)$$

The corresponding expansion for a trough-focused wave group is

$$\eta_{tr} = -\sum_i a_i + \sum_{i,j} c_{ij}a_i a_j - \sum_{i,j,k} c_{ijk}a_i a_j a_k + \sum_{i,j,k,l} c_{ijkl}a_i a_j a_k a_l. \quad (9)$$

The even-order terms in these expansions have the same sign, whereas the odd-order terms are of opposite sign; this implies that the large-scale changes in group structure can

only be consistent with odd-order nonlinear interactions. The computational domain has sufficient resolution to accurately model fifth-order wave-wave interactions (see Section 2.3), so the third-order resonant interactions are accurately represented. Comparisons with simulations using the G-operator truncated at G_2 show that all the main group dynamics are captured by third-order effects. Therefore these global changes to the wave groups appear to be examples of the combined third-order near-resonant interactions of Benjamin and Feir [6] and the resonant interactions of Phillips [4].

The strong nonlinearity shown by the contraction of the wave group in the mean wave direction should be apparent in the temporal variation of the kinetic and potential energies. The linear evolution of a wave group gives an equipartition between kinetic and potential energy. However, for large amplitude wavetrains Lighthill [34] showed that their average values diverge at high wave steepness with the average kinetic energy taking on a slightly greater value than the average potential energy. At the nonlinear focus time in our simulations the average kinetic energy has increased by about 1% with a corresponding decrease in the average potential energy; there is a return towards energy equipartition when the group is well dispersed beyond the focus time.

The symmetry property of the crest-focused and trough-focused evolutions permits their difference to be computed giving a new meaningful signal, which may be used to analyse the changes in the wave group dynamics during nonlinear evolution. This differencing procedure defines a signal, which we refer to as the locally linearised surface elevation, $\eta_{\mathrm{odd}}(x,y,t)$,

$$\eta_{\mathrm{odd}} = (\eta_{\mathrm{cr}} - \eta_{\mathrm{tr}})/2. \tag{10}$$

In terms of the general perturbation expansions for the crest-focused wave group, Eq. (8), and the trough-focused wave group, Eq. (9), the locally linearised surface elevation is given by

$$\eta_{\mathrm{odd}} = \sum_i a_i + \sum_{i,j,k} c_{ijk} a_i a_j a_k + O(a^5). \tag{11}$$

This represents a signal in both space and time with all the even-order bound wave structure removed, thus leaving the free wave components and the odd-order bound wave harmonics. Inspection of the locally linearised wave amplitude spectra (Fig. 13, which is described in Section 4) shows only a weak contribution from the third harmonics. Therefore this locally linearised wave group may be used to visualize the dynamic changes to the aspect ratio of the wave group envelope without the dominant interference from the second-order bound wave structure. After the first 10 time periods of evolution the departure of the nonlinear evolution from the linear solution is small (Fig. 7(a) and (b)); the overall shapes are similar. However, the peak of the nonlinear envelope is beginning to move towards the front of the group, accompanied by a slight contraction of the group along the mean wave direction. It appears that there is an initial delay period, while linear dispersion brings the waves together, before a critical concentration of energy can trigger significant nonlinear wave–wave interactions. Dramatic changes take place to the group shape in the following 10 time periods; linear dispersion and nonlinearity produce a group that is most compact in the transverse direction four time periods before the linear focus time and from this point there is a rapid expansion relative to the linear solution. At the nonlinear focus time there is a major contraction at the front of the group, along the mean wave direction, resulting in the dramatic form of the peak crest (Fig. 7(c) and (d)). In a sense this is balanced by the vigorous expansion of the group in the transverse direction, giving a significantly more long-crested focused event. Indeed, comparison of the 10 m contours reveals that the transverse extent of the tallest peak is 2.5 times wider in the nonlinear group than in the linear group. This rather thin, but long crest sustains a height of at least 10 m across a distance of 230 m. The nonlinear group remains locally much more long-crested beyond the focus point, while a group of waves is left well behind the peak crest (Fig. 7(e) and (f)). Rapid nonlinear interactions have formed a focused group which is locally wider in the transverse direction than it is in the mean wave direction, this represents a reversal in the aspect ratio of the group in comparison with the linear solution.

3.3. Quantifying changes to group shape

The dramatic changes that take place during the nonlinear evolution of a steep focused wave group have been shown to be dependent on the group properties of the wave field. The wave group described in Section 3.1 has been simulated for a range of input wave steepness. Therefore this section considers some approximate measures for these properties, such as amplitude and bandwidths in the two horizontal dimensions, and how they change with input wave steepness and time.

3.3.1. Amplitude changes

The maximum surface elevation reached during each simulation is shown as a function of steepness in Fig. 8 for the nonlinear focusing to form a tall crest, η_{cr}, and to form a deep trough, η_{cr}; the linear values, A, are given as a guide to the degree of nonlinearity. A comparison of the crest-focused values to the linear solution reveals little change in maximum elevation at low wave steepness and an appreciable gain, about 20%, in elevation only for the steepest groups. However, a comparison of the peak of the locally linearised signal, defined by Eq. (10), to the linear solution shows only a very slight increase, about 6%, in elevation for the steepest groups. As the third-order bound wave contributions appear to be negligible even for the steepest wave groups (Fig. 13, which is described in Section 4), then the application of the second-order solution of Longuet-Higgins [32] to the locally linearised signal will essentially return the crest-focused surface elevation. Therefore, only for the steepest groups is there extra elevation beyond a second-order prediction based on the underlying free wave components at the nonlinear focus. This minimal gain in elevation, at least for the particular choice of initial conditions, is in stark contrast to the behaviour of unidirectional focused

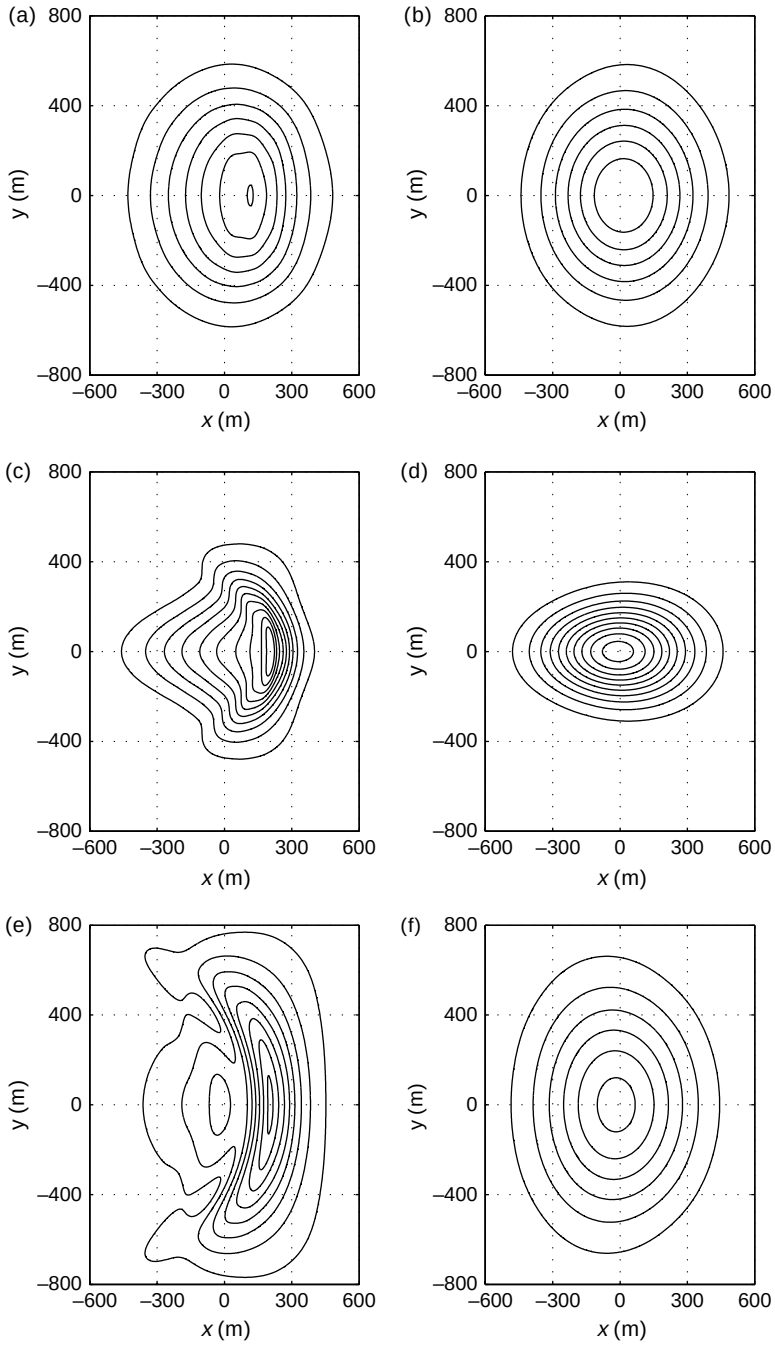

Fig. 7. Amplitude contours of the envelope of the surface elevation, $Ak_p = 0.3$: (a), (b) $t = -9.0T_p$; (c), (d) $t = 1.3T_p$; (e), (f) $t = 10.9T_p$. The left hand column gives the signal (η_{odd}), locally linearised from the nonlinear evolution; the right hand column gives the linear evolution. The contours are given in 1.0 m intervals above mean sea level starting at $\eta = 1.0$ m. The frame of reference is moving at the linear group velocity.

wave groups, which can produce large gains, up to about 20%, above a second-order solution (for example in the experiments of Baldock et al. [18]).

3.3.2. Bandwidth changes

The large contraction in the mean wave direction may be measured by a bandwidth, based on a local approximation to the wave group envelope. The shape of the linear focused event is almost identical to a simple Gaussian envelope multiplied by the carrier wave, Eq. (7). As the main interest is in dynamical effects beyond a second-order description of the sea surface, the locally linearised signal will be used to assess these changes. The envelope of the locally linearised signal, $A(x)$, is considered, so that the interference effect as crests pass through the wave group can be avoided, and fitted to a local Gaussian envelope along the mean wave direction

$$A(x) \approx \bar{A} e^{-(1/2)S_x^2 x^2}, \tag{12}$$

where $\bar{A}$ is the peak value of the locally linearised envelope.

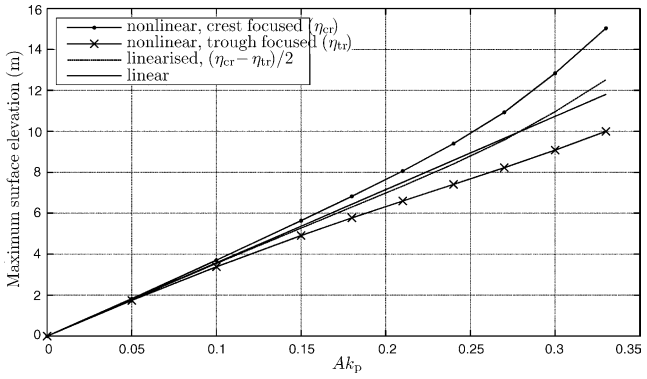

Fig. 8. Maximum surface elevation at focus for a range of input wave group steepness.

This local measure for the bandwidth in the mean wave direction may be tracked with time (Fig. 9) to highlight the rapid contraction of the group around the peak crest. Initially all the wave groups considered are well dispersed and so the bandwidth is small. For the linear solution this value increases slowly up to the focus time, when all the wave components are in phase, giving $S_x = 0.00464\ \mathrm{m}^{-1}$ as is expected from Section 2.2. For the nonlinear evolution there is little departure from the linear solution until about 12 time periods from focus; after this time there is a rapid increase in the local bandwidth, becoming more rapid with increasing wave steepness, which is consistent with the envelopes of Fig. 7. This bandwidth measure suggests that the peak crest is most compact slightly after focus for the steepest groups and becomes most compact at later times for groups of intermediate steepness. For the wave group of steepness $Ak_p = 0.3$, analysed in Section 3.2, the local bandwidth has increased by a factor of 3.3 (Fig. 10). Beyond the focus time there is a reduction in the bandwidth as the groups eventually disperse, but this reduction is slow relative to the focusing of the group. The variation of the maximum of the local bandwidth against the square of the input wave steepness is shown in Fig. 10.

The large expansion in the transverse direction may be measured by a local spreading angle determined in a similar way to the inline wave kinematics factor used by offshore designers

$$f = \cos\theta_u = \frac{U_{\mathrm{inline}}}{U_{1D}}, \tag{13}$$

which accounts for how the presence of spreading reduces fluid particle velocities in comparison to a linear unidirectional model (see [35]). In an analogous manner we define a local spreading angle

$$\theta = \cos^{-1}\left(\frac{\eta_{\mathrm{inline,env}}}{\eta_{\mathrm{env}}}\right), \tag{14}$$

which gives a local measure of how long-crested the wave group is at a particular spatial location. This local spreading angle is calculated from the locally linearised surface elevation in order to isolate the underlying dynamical effects that alter the group shape, and envelopes are used to remove the interference effect of crests passing through the group. This parameter, like the measure for the bandwidth in the mean wave direction local to the peak crest, is smoothed by taking a running average over a time period.

This local spreading angle, Eq. (14), is evaluated in the following manner. The Fourier series representation of a wave group is given by

$$\eta(x,y) = \sum_{m=0}^{M}\sum_{n=0}^{N} a_{mn}\cos(k_{x_m}x + k_{y_n}y + \Phi_{mn}). \tag{15}$$

Each wave component makes a contribution to the surface elevation of the group along the mean wave direction ($y=0$), and for each component propagating at an angle θ to the mean wave direction there is an equal contribution from a wave

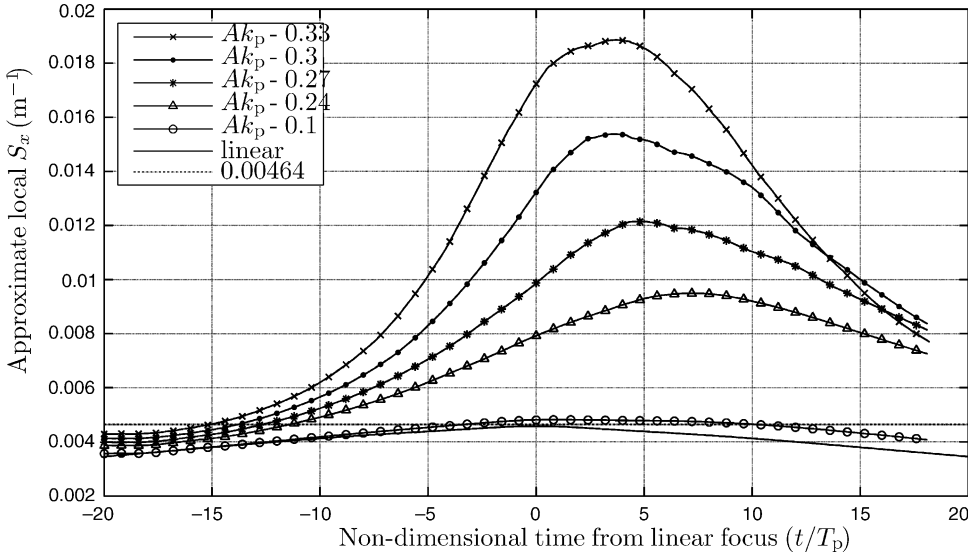

Fig. 9. Variation of an approximate local bandwidth in the mean wave direction with non-dimensional time from linear focus for a range of wave steepness. The bandwidth of the linear focused group is $S_x = 0.00464\ \mathrm{m}^{-1}$.

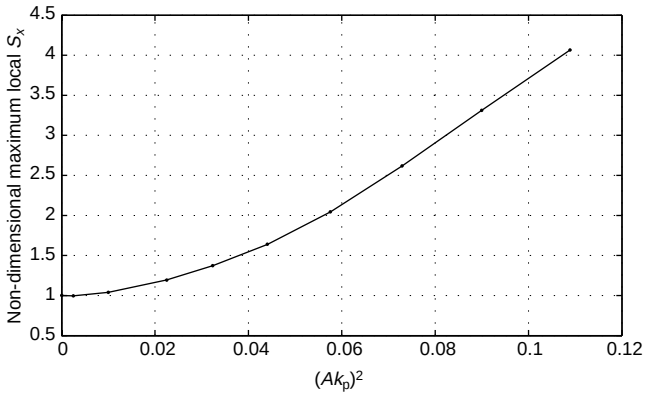

Fig. 10. Variation of a non-dimensional maximum local bandwidth in the mean wave direction with the square of the wave steepness.

component propagating at an angle of $-\theta$. So, resolving along the mean wave direction, the contributions from all the wave components give the inline 'surface elevation'

$$\eta_{\text{inline}}(x,y=0) = \sum_{m=0}^{M}\sum_{n=0}^{N} a_{mn}\cos(k_{x_m}x + \Phi_{mn})\cos\theta_{mn}, \qquad (16)$$

where

$$\cos\theta_{mn} = k_{x_m}(k_{x_m}^2 + k_{y_n}^2)^{-1/2}.$$

This quantity and its Hilbert transform, $\eta_{H_{\text{inline}}}$, may be used to calculate the envelope of the inline surface elevation

$$\eta_{\text{inline,env}}(x,y=0) = \sqrt{\eta_{\text{inline}}^2 + \eta_{\text{H}_{\text{inline}}}^2}. \qquad (17)$$

This quantity has a simple physical interpretation, it is the maximum horizontal fluid particle displacement at the surface in the mean wave direction based on a linear wave model. In order to determine a spreading angle local to the peak crest the maximum value of the envelope of the inline surface elevation (located at $x=\bar{x}$) is compared to the value of the envelope for the original surface at the location of this maximum.

This local measure for the spreading angle may be tracked with time (Fig. 11) to highlight the rapid expansion of the

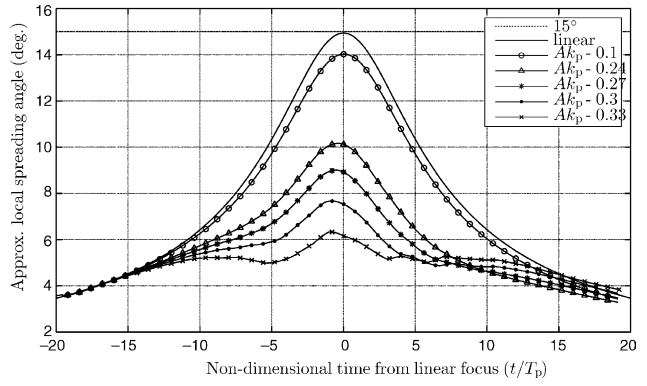

Fig. 11. Variation of an approximate local spreading angle with non-dimensional time from linear focus for a range of wave steepness. The spreading angle of the linear focused group is $\theta=15°$.

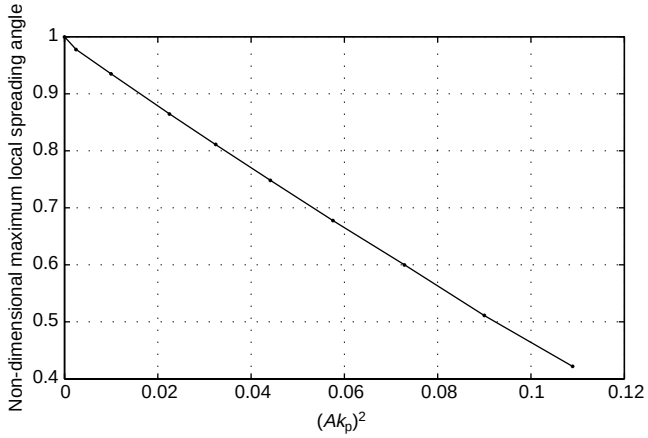

Fig. 12. Variation of a non-dimensional maximum local spreading angle with the square of the wave steepness.

group local to the peak crest. Any group well dispersed in frequency and direction will appear, at least locally, like a plane wave, and so all the wave groups have an initially low spreading angle. Under linear evolution this value increases up to the value of 15°, equal to the initial rms spreading angle (see Section 2.2), at the focus time. For the nonlinear evolution there is little departure from the linear solution until about 12 time periods from focus; after this time the rate of increase in the spreading angle slows before increasing again until a maximum angle is reached just before the nonlinear focus time. As the wave group steepness increases there is a reduction in the maximum spreading angle of the group, which is consistent with the locally more planar front of the peak crest of Fig. 1. For the wave group of steepness $Ak_p=0.3$, analysed in Section 3.2, the local spreading angle has decreased by a factor of 2 (Fig. 12) to approximately 8°. Beyond the focus time there is a rapid reduction in the spreading angle as the groups become so dispersed that it is impossible to distinguish between the linear and nonlinear groups based on this local measure, but globally there remain noticeable differences in the group shape (Fig. 7(e) and (f)). A comparison of the maximum of the local spreading angle with the square of the input wave steepness (Fig. 12) suggests that the expansion of the group local to the peak crest is consistent with a dominant third-order process. It is worth noting that there is only one dominant nonlinear process in the transverse direction, which is the expansion of the group. Therefore any wave component that does not participate in this process makes a negligible contribution to the local spreading angle. Along the mean wave direction, there are two nonlinear processes: the contraction of the group for the strongly interacting components, and the splitting of the group as the components not participating in the main interaction get left behind. Wave components, in the trailing group, which partially overlap the peak crest will contribute to the local bandwidth and so will contaminate this parameter. This local parameter is a true measure of the contraction of the group only at high input steepness, when the contraction process dominates the behaviour along the mean wave direction.

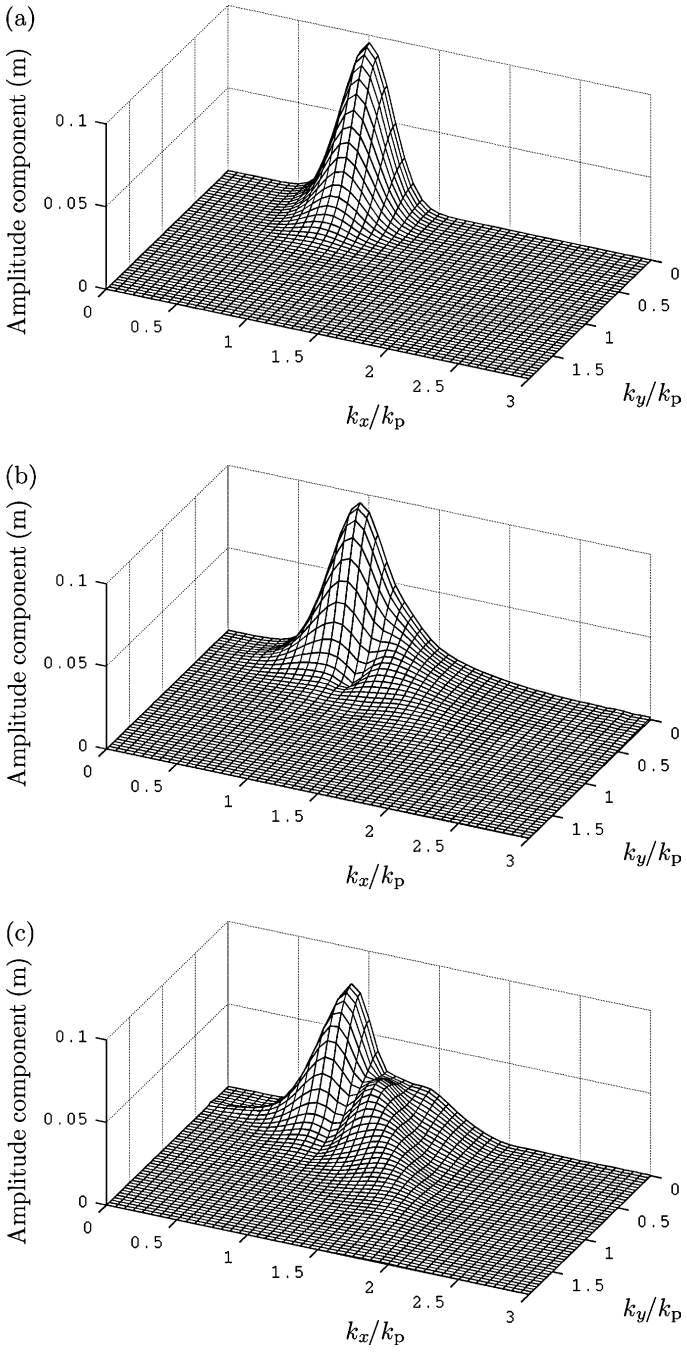

Fig. 13. Amplitude spectra of the locally linearised signal, $Ak_p=0.3$: (a) $t=-20T_p$; (b) nonlinear focus; (c) $t=20T_p$.

4. Spectral evolution

It is reasonable to expect that the large nonlinear changes to the group shape will result in significant changes in the amplitude spectra for these wave groups. The amplitude spectrum of the locally linearised surface elevation is considered, as the dominant second-order bound wave structure has been removed. This gives an approximation to the underlying free waves at any time and returns the underlying linear input spectrum when applied to the second-order initial condition. For a group evolving linearly there are no mechanisms by which energy may be transferred between wave components and so the initial spectrum (Fig. 13(a)) remains unaltered with time. However, there has been considerable energy transfer away from the spectral peak at the point of nonlinear focus (Fig. 13(b)). Close to the k_x-axis (corresponding to the mean wave direction) there is a broadening of the peak, particularly noticeable up to $k_x=2k_p$, and a contraction in the k_y-direction (corresponding to the transverse direction), which are consistent with the changes in the shape of the envelope (Fig. 7). A small amount of energy has been transferred to even higher wavenumbers, beyond $k_x=3k_p$, as noted from the slight step where the spectrum is only shown up to $k_x=3k_p$. This large transfer of energy to high wavenumbers was observed in the wave basin experiments of Johannessen and Swan [16] and later shown to correspond to freely propagating waves in their numerical simulations [20] (see also Bateman [19]). Large energy transfers take place well after the focus time, but twenty time periods later (Fig. 13(c)) the group behaves sufficiently linearly for the spectral changes to be considered permanent. There is a return of energy from the highest wavenumbers, $k_x>2k_p$, close to the k_x-axis and further energy has been transferred to high wavenumbers up to $k_x=2k_p$. Two new structures have developed from the low and high wavenumber sides of the spectral peak. A low level ridge now extends from the peak region to the k_y-axis, and so a small amount of energy must be sent out sideways from the extreme event. A secondary peak has formed at ($k_x=1.2k_p$, $k_y=0.28k_p$), from which a high level ridge extends to higher wavenumbers. This ridge makes a distinct angle with the k_x-axis of about 55°, indicating a strong directional preference for the transfer of energy. These two ridges show a strong likeness to similar features seen in ensemble-averaged spectra from simulations of a random sea state performed by Dysthe et al. [13] using a modified NLS equation. The ridge on the high wavenumber side of the spectral peak has also been seen by Bateman [19] in his NewWave simulations based on a truncated JONSWAP spectrum with a small directional spread.

The large energy transfers to low and high wavenumbers cause a downshift in the position of the peak of the amplitude-wavenumber spectrum, which is not possible for linear evolution. The overall permanent downshift of the spectral peak in wavenumber is about 10% for the steepest groups, an effect which has also been observed for non-breaking spread seas by Trulsen and Dysthe [36] and Dysthe et al. [13] in their simulations of a modified NLS equation. However, this downshifting of the position of the spectral peak should not be confused with the downshifting that occurs for the development of wave spectra over longer time scales. This latter phenomenon sees the whole spectrum shift to lower wavenumbers and dissipation due to wave breaking is generally believed to be an important mechanism in this process (a brief review is given by Dias and Kharif [37]).

5. Conclusions

Steep directionally spread focused wave groups on deep water have been simulated to analyse their spatial structure and

identify nonlinear dynamic processes in their evolution. For the steepest wave groups, based on a spectral peak model, a prominent peak crest forms at the front of the group with an elevation and transverse width that are highly suggestive of a 'wall of water'. This structure is significantly different to the expected shape of an extreme event based on linear dispersion, even after accounting for the second-order crest-trough asymmetry. The formation of these events is controlled by the group properties of the underlying wave field, as the evolution of an extreme crest is essentially identical to the evolution of an extreme trough. As the group focuses, dramatic and rapid changes to the group shape are caused by two nonlinear processes close to the focus time. There is a strong contraction of the group along the mean wave direction, which appears to be balanced by a strong expansion of the group in the transverse direction. Three group properties — amplitude, bandwidth in the mean wave direction and bandwidth in the transverse direction — appear to be important in understanding the behaviour of steep focused wave groups, with the bandwidth changes being consistent with third-order near-resonant [6] and resonant [4] processes (of Benjamin and Feir, and Phillips respectively). In work currently in preparation, we will compare the results of 'fully' nonlinear simulations to those from simpler nonlinear evolution equations such as the nonlinear Schrödinger equation [14].

The unidirectional focusing of wave groups leads to a dramatic contraction of the group and significant gains in the peak surface elevation, well beyond second-order theory. This contraction process is also present in the physics of spread sea wave groups, but there is now an additional process — the expansion of the group in the transverse direction, that is not possible in unidirectional physics. This expansion process appears to be the reason for the absence of large amplitude gains for the focusing of spread sea wave groups. These strongly nonlinear processes lead to permanent net changes to the amplitude spectrum of a spread sea wave group. Overall, the physics of directionally spread wave groups is very different to that for unidirectional groups: wave spreading is crucial in understanding the behaviour of realistic extreme wave groups. The nonlinear behaviour of such directionally spread groups close to focus exhibits many of the hallmarks of 'freak' waves. Although the calculations presented here are for groups of fixed shape (spectral bandwidth and directionality), these parameters are chosen to be representative of those likely to occur for large waves on the open sea. Thus, the shape changes should be a robust and observable feature.

It may be that significant extra elevation, such as commonly occurs in unidirectional wave tank experiments and simulations, occurs very rarely in the open sea — only when a much less directionally spread and frequency focused wave group forms by chance.

Acknowledgements

The authors are grateful to Dr William Bateman and Dr Chris Swan of the Department of Civil and Environmental Engineering, Imperial College, London for generously allowing unrestricted use of their spread sea implementation of the Craig and Sulem scheme. R.H.G. is grateful for the financial support of the Engineering and Physical Sciences Research Council of the UK (EPSRC), through their doctoral studentship programme.

References

[1] Haver S, Andersen OJ. Freak waves: rare realizations of a typical population or typical realizations of a rare population? In: Proceedings of the tenth international offshore and polar engineering conference (ISOPE), Seattle, USA, vol. 3; 28 May–2 June 2000. p. 123–30.
[2] Jonathan P, Taylor PH, Tromans PS. Storm waves in the northern north sea. In: Proceedings of the seventh international conference behaviour of offshore structures (BOSS), Massachusetts Institute, USA, 12–15 July 1994, vol. 2. p. 481–94.
[3] Kharif C, Pelinovsky E. Physical mechanisms of the rogue wave phenomenon. Eur J Mech B Fluids 2003;22:603–34.
[4] Phillips OM. On the dynamics of unsteady gravity waves of finite amplitude, part 1 the elementary interactions. J Fluid Mech 1960;9: 193–217.
[5] Lighthill MJ. Contributions to the theory of waves in non-linear dispersive systems. J Inst Math Applics 1965;1:269–306.
[6] Benjamin TB, Feir JE. The disintegration of wave trains on deep water, part 1. Theory. J Fluid Mech 1967;27:417–30.
[7] Peregrine DH. Water waves, nonlinear Schrödinger equations and their solutions. J Austral Math Soc B 1983;25:16–43.
[8] Dysthe KB, Trulsen K. Note on breather type solutions of the NLS as models for freak-waves. Phys Scripta T 1999;82:48–52.
[9] Yuen HC, Lake BM. Nonlinear dynamics of deep-water gravity waves. Adv Appl Mech 1982;22:67–229.
[10] Dysthe KB. Note on a modification to the nonlinear Schrödinger equation for application to deep water waves. Proc R Soc Lond A 1979;369:105–14.
[11] Trulsen K, Dysthe KB. A modified nonlinear Schrödinger equation for broader bandwidth gravity waves on deep water. Wave Motion 1996;24: 281–9.
[12] Trulsen K, Kliakhandler I, Dysthe KB, Velarde MG. On weakly nonlinear modulation of waves on deep water. Phys Fluids 2000;12:2432–7.
[13] Dysthe KB, Trulsen K, Krogstad HE, Socquet-Juglard H. Evolution of a narrow-band spectrum of random surface gravity waves. J Fluid Mech 2003;478:1–10.
[14] Lo EY, Mei CC. Slow evolution of nonlinear deep water waves in two horizontal directions: a numerical study. Wave Motion 1987;9:245–59.
[15] Osborne AR, Onorato M, Serio M. The nonlinear dynamics of rogue waves and holes in deep-water gravity wave trains. Phys Lett A 2000;275:386–93.
[16] Johannessen TB, Swan C. A laboratory study of the focussing of transient and directionally spread surface water waves. Proc R Soc Lond A 2001; 457:971–1006.
[17] Taylor PH, Haagsma IJ. Focussing of steep wave groups on deep water. In: Proceedings of the international symposium: waves–physical and numerical modelling, University British Columbia, Vancouver, Canada; 21–24 August 1994. p. 862–70.
[18] Baldock TE, Swan C, Taylor PH. A laboratory study of nonlinear surface waves on water. Phil Trans R Soc Lond A 1996;354:649–76.
[19] Bateman WJD. A numerical investigation of three dimensional extreme water waves. PhD Thesis. Imperial College, University of London, UK; 2000.
[20] Johannessen TB, Swan C. On the nonlinear dynamics of wave groups produced by the focusing of surface-water waves. Proc R Soc Lond A 2003;459:1021–52.
[21] Craig W, Sulem C. Numerical simulation of gravity waves. J Comp Phys 1993;108:73–83.
[22] Bateman WJD, Swan C, Taylor PH. On the efficient numerical simulation of directionally-spread surface water waves. J Comp Phys 2001;174:277–305.
[23] Lindgren G. Some properties of a normal process near a local maximum. Ann Math Stat 1970;41:1870–83.

[24] Boccotti P. Some new results on statistical properties of wind waves. Appl Ocean Res 1983;5:134–40.
[25] Boccotti P, Barbaro G, Mannino L. A field experiment on the mechanics of irregular gravity waves. J Fluid Mech 1993;252:173–86.
[26] Boccotti P. A general theory of three-dimensional wave groups part 1: the formal derivation. Ocean Eng 1997;24:265–80.
[27] Tromans PS, Anaturk A, Hagemeijer P. A new model for the kinematics of large ocean waves—application as a design wave. In: Proceedings of the first international offshore and polar engineering conference (ISOPE), Edinburgh, UK, vol. 3, 11–16 August 1991. p. 64–71.
[28] Jonathan P, Taylor PH. On irregular non-linear waves in a spread sea. J Offshore Mech Arctic Eng 1997;119:37–41.
[29] Hasselmann K, Barnett TP, Bouws E, Carlson H, Cartwright DE, Enke K, et al. Measurement of wind-wave growth and swell decay during the joint North Sea wave project (JONSWAP). Deutsches Hydrographisches Zeitschrift 1973;12(Suppl. A8).
[30] Donelan MA, Hamilton J, Hui WH. Directional spectra of wind-generated waves. Phil Trans R Soc Lond A 1985;315:509–62.
[31] Ewans KC. Observations of the directional spectrum of fetch-limited waves. J Phys Oceanogr 1998;28:495–512.
[32] Longuet-Higgins MS. The effect of non-linearities on statistical distributions in the theory of sea waves. J Fluid Mech 1963;17:459–80.
[33] Dyachenko AI, Zakharov VE. Modulation instability of Stokes wave → freak wave. JETP Lett 2005;81:255–9.
[34] Lighthill MJ. Waves in fluids. Cambridge: Cambridge University Press; 1978.
[35] Tucker MJ, Pitt EG. Waves in ocean engineering. Oxford, UK: Elsevier; 2001.
[36] Trulsen K, Dysthe KB. Frequency downshift in three-dimensional wave trains in a deep basin. J Fluid Mech 1997;352:359–73.
[37] Dias F, Kharif C. Nonlinear gravity and capillary-gravity waves. Annu Rev Fluid Mech 1999;31:301–46.